ISSN 0006-2979, Biochemistry (Moscow), 2024, Vol. 89, No. 5, pp. 862-871 © Pleiades Publishing, Ltd., 2024.

REVIEW

Antigenic Cartography of SARS-CoV-2

Ekaterina A. Astakhova[1,2,a]*, Alexey A. Morozov[1,2], Julia D. Vavilova[3], and Alexander V. Filatov[1,2]

[1]*National Research Center Institute of Immunology, Federal Medical Biological Agency of Russia, 115522 Moscow, Russia*

[2]*Department of Immunology, Faculty of Biology, Lomonosov Moscow State University, 119234 Moscow, Russia*

[3]*Shemyakin–Ovchinnikov Institute of Bioorganic Chemistry, Russian Academy of Sciences, 117997 Moscow, Russia*

[a]*e-mail: ast_kat@mail.ru*

Received November 7, 2023
Revised January 14, 2024
Accepted January 17, 2024

Abstract—Antigenic cartography is a tool for interpreting and visualizing antigenic differences between virus variants based on virus neutralization data. This approach has been successfully used in the selection of influenza vaccine seed strains. With the emergence of SARS-CoV-2 variants escaping vaccine-induced antibody response, adjusting COVID-19 vaccines has become essential. This review provides information on the antigenic differences between SARS-CoV-2 variants revealed by antigenic cartography and explores a potential of antigenic cartography-based methods (e.g., building antibody landscapes and neutralization breadth gain plots) for the quantitative assessment of the breadth of the antibody response. Understanding the antigenic differences of SARS-CoV-2 and the possibilities of the formed humoral immunity aids in the prompt modification of preventative vaccines against COVID-19.

DOI: 10.1134/S0006297924050079

Keywords: antigenic cartography, SARS-CoV-2, COVID-19, breadth of virus-neutralization

INTRODUCTION

Since the beginning of the COVID-19 pandemic, more than 40 variants of SARS-CoV-2 have emerged, of which more than 10 belong to the Omicron family (https://www.who.int/activities/tracking-SARS-CoV-2-variants, https://covariants.org/, 01.09.2024). SARS-CoV-2 variants differ in contagiousness, nature of infection caused, and some other epidemiological characteristics [1-3]. There are several ways to classify viral variants. The most common is construction of phylogenetic trees of viral variants and isolates based on sequencing data [4]. The phylogenetic trees reveal the evolution of viral variants and routes of their spread. However, such classification provides only an indirect information with regard to antigenicity [5]. Obviously, not all mutations are equally important. The most intriguing of them are mutations in the surface spike protein (S protein) located within the domains directly involved in the interaction with host cell receptors or in the virus fusion with the host cell. The most important mutations are those allowing the virus to escape neutralizing antibodies formed after vaccination or previous infections. These mutations constitute the antigenic profile of a viral variant.

Quantification of antigenic differences presents certain difficulties. The arithmetic sum of mutations cannot be a measure of antigenic differences. Some of mutations are more immunogenic, while others are less; they may occur in functionally important regions of the antigens or happen far from them. This problem can be solved using the method of antigenic mapping that was first applied in the study of influenza virus [6] and is now increasingly used to monitor the emergence of new SARS-CoV-2 variants and to assess their antigenicity. Here, we reviewed the published data on the antigenic properties of SARS-CoV-2 obtained using antigenic maps.

Abbreviations: AU, antigenic unit; WT, wild type.

* To whom correspondence should be addressed.

STEPS IN CONSTRUCTING ANTIGENIC MAPS

Determining the antigenic characteristics of the virus using antigenic maps begins with serological tests [7]. While hemagglutination inhibition (HI) test is commonly used for the influenza virus, the gold standard for SARS-CoV-2 is the live virus neutralization test (cVNT, conventional virus-neutralization test). Due to the increased safety requirements for working with a live virus, cVNT is often replaced with a test using virus-like particles pseudotyped with the coronavirus S protein (pVNT, pseudovirus-based virus-neutralization test). A high level of correlation between the cVNT and pVNT results has been repeatedly shown [7-10]. These tests provide a rich set of multidimensional data that, due to their large volume, are difficult to interpret.

Biological science has previously encountered similar multidimensional problems, for example, when interpreting transcriptomics data or data obtained by multicolor flow cytometry [11-13]. The t-SNE (t-stochastic neighborhood embedding) and UMAP (uniform manifold approximation and projection) algorithms were developed to reduce the dimensionality of data [14, 15], which made it possible to represent multidimensional data on a two-dimensional plane. The advantage of these algorithms is preservation of proximity between the points by taking into account the distances between them in a multidimensional space. Antigenic maps are constructed using a method based on the principle of multidimensional scaling (MDS) [16], which in its algorithms is close to the traditional principal component analysis (PCA). The advantage of MDS is that the distance between the points visualized on a plane closely matches the distance between them in the multidimensional space.

The construction of antigenic maps begins with a creation of tables with sera shown in the columns, virus variants – in the rows, and neutralization titers – at the intersection. Next stage, neutralization titers are converted into antigenic distances (https://acorg.github.io/Racmacs/articles/intro-to-antigenic-cartography.html, 09.04.2023). The higher the serum neutralization titer relative to the antigen, the smaller the antigenic distance between them. Next, the MDS method is applied and the data are visualized on a plane.

Antigenic maps display both antigens (virus variants) and sera. The distance between a serum and an antigen directly depends on the antigenic distance. Variants with similar antigenic properties are located next to each other, forming a cluster. For example, the wild-type (WT) coronavirus co-clusters with the Alpha, Beta, and Gamma variants [17], but, as a rule, is far removed from the Omicron variants (Fig. 1).

The antigenic evolution of a virus differs from its genetic evolution, since different mutations make an unequal contribution to changes in its antigenic characteristics. For example, the E484K/Q mutation is the most significant for the antigenic differences between the Beta, Gamma, Kappa, and Mu variants relative to WT, while the L452R/Q mutation is decisive for the Delta, Epsilon, and Lambda variants, although other mutations are also present in these variants [18, 19].

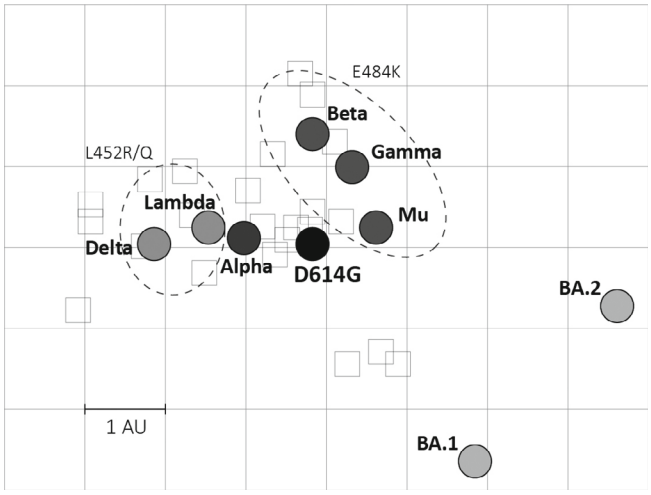

Fig. 1. Example of a SARS-CoV-2 antigenic map (adapted from [18]). Circles, locations of individual antigens; squares, locations of individual sera; dotted lines, variants with common specified substitutions.

Significant changes in the antigenic properties of a new virus variant lead to the inability of antibodies that neutralize the previous variant to neutralize the new one. In this case, first, the new variant will be located at a great distance from the previous variants on the antigenic map. Second, there will be no sera located on the map between the studied variants.

PREVIOUS EXPERIENCE OF THE IMMUNE SYSTEM INFLUENCES THE POSITION OF A VIRAL VARIANT ON THE ANTIGENIC MAP

At first glance, it may seem that the location of viral variants on the antigenic map depends solely on the number and quality of amino acid substitutions. However, this is not entirely true. Prior exposure of the immune system to either SARS-CoV-2 infection or vaccination can significantly change the degree of neutralization of viral variants and, therefore, influence the appearance of antigenic maps. Indeed, sera from infected laboratory animals or recovered people, vaccinated volunteers, and individuals with the hybrid immunity ultimately produce different antigenic maps [20-22]. Thus, the position of a viral variant on the antigenic map, and, consequently, the distance between the variants, depend not only on the structure or composition of their immunodominant epitopes, but also on the source of sera that was used to construct the map.

QUANTITATIVE ESTIMATION OF ANTIGENIC DISTANCES BETWEEN VIRUS VARIANTS

Antigenic maps are widely used to make decisions about changing the strain of the influenza virus vaccine. Smith et al. [6] retrospectively analyzed the evolution of the influenza virus from 1968 to 2003 and showed that vaccine strains changed when the new variant was 2 or more antigenic units (AU) away from the previous vaccine strain, which was used to define the "sufficiency" of antigenic differences between the viruses for updating a vaccine strain. For SARS-CoV-2, this criterion has not yet been clearly determined. However, after constructing the first maps with Omicron BA.1, it was noticed it was located "like a lonely island in the middle of the ocean" on the antigenic map of SARS-CoV-2 (https://spectrum.ieee.org/omicron-covid-variant#toggle-gdpr, 09.04.2023), i.e., was far from the pre-Omicron variants. This observation provided a good explanation for the spread of breakthrough infections among vaccinated donors and prompted consideration of the necessity to update the vaccine strain.

At present, significant antigenic differences between the WT coronavirus and Omicron family variants cause no doubt. These differences range from 3 to 9 AU depending on the variant [18, 20-25], where one AU corresponds to a twofold serum dilution. The most distant from D614G are the variants BQ.1.1, BM.1.1.1 and XBB.1, XBB.2, BN.1.3.1 [22, 25]. The distance between these variants and the D614G is more than 6 AU. The variants of the Omicron family are antigenically distant not only from pre-Omicron variants, but also from each other [22, 25, 26]. For example, XBB.1 and BM.1.1.1 are located at a distance of about 6 AU from each other on the Omicron antigenic map [25].

Unfortunately, exact determination of antigenic distances is not a straightforward procedure. The antigenic distances between the same variants determined in different studies may differ (table) likely due to different methods for obtaining the samples. Standardization of serum collection procedure and testing conditions can lead to a more precise quantification of antigenic variances.

APPLICATION OF ANTIGENIC MAPPING FOR DETERMINING THE OPTIMAL VACCINE STRAIN

Once it is discovered that a new variant is antigenically distant from the previous one, the question arises of which particular variant should be used for

Antigenic distances between D614G and SARS-CoV-2 variants

No.	Serum source	Antigenic distance between D614G and variant						References
		Alpha	Beta	Delta	BA.1	BA.2	BA.4/5	
1	Syrian hamsters, 14 days after double i.n. SARS-CoV-2 administration	0.8	1.1	0.7	4.4	3.7	4.8	[22]
2	Syrian hamsters, 26 days after i.m. SARS-CoV-2 injection	0.8	1.3	1.7	4.7	4.0	ND	[18]
3	Syrian hamsters, 26 days after i.m. SARS-CoV-2 injection	1.4	0.6	1.5	6.2	5.6	5.0 (BA.5)	[25]
4	Recovered donors	0.9	2.0	1.2	4.7	4.0	ND	[21]
5	Vaccinated (mRNA-1273, BNT162b or ChAdOx-S1) donors	0.4	2.2	1.7	5.9	ND	ND	[21]
6	Recovered donors	0.6	3.7	1.4	7.0	6.3	5.8	[20]
7	Recovered or vaccinated (mRNA-1273) donors	0.5	3.8	2.2	5.6	5.3	6.7	[19]
8	Recovered or vaccinated (mRNA-1273 ×2*, BNT162b ×2, AZD1222 ×2 or AZD1222/BNT162b) donors	0.8	2.1	1.5	5.5	3.3	4.2 (BA.5)	[27]

Note: i.n., intranasal; i.m., intramuscular injection; ND, not determined; * double homologous vaccination.

the next vaccine [28]. For this purpose, a "basic" antigenic map is built. Laboratory animals (most often, Syrian hamsters or mice) are infected with a potential vaccine strain, and the extent to which the resulting sera cross-neutralize the variants of interest is determined.

It was shown [17] that sera from mice infected with the Gamma variant also neutralized the WT and Beta variants (these sera are located between the WT, Beta, and Gamma antigens on the antigenic map). At the same time, sera from the mice infected with the Beta variant did not neutralize WT and Gamma.

The focus of current research is to identify a suitable SARS-CoV-2 vaccine strain from the Omicron family. In [29], K18-hACE2 sera from the mice infected with BA.1 neutralized BA.1 to the greatest extent, but also showed broad cross-reactivity with BA.2 and BA.2.12.1. Sera from the mice infected with BA.5 neutralized BA.2 and BA.2.12.1 and, to a lesser extent, BA.4.6 and BA.5 and were located on the antigenic map mainly close to BA.2.12.1, being distant from BA.5 at 1 or more AU. Another study showed that sera from the BA.5-infected hamsters neutralized BA.2 and BQ.1.1 and, to a lesser extent, BM.1.1.1. None of the sera neutralized XBB.1 [25]. Despite the antigenic similarity of BA.5 and BQ.1.1, the authors questioned whether inclusion of BA.5 in a bivalent vaccine would result in a sufficient level of cross-response against BQ.1.1 due to the fact that the two variants do not cluster with each other (distance of more than 3 AU).

As confirmed in [30-32], immunization of people with a bivalent vaccine based on BA.5 did not induce significant neutralization of BA.2.75.2, BQ.1.1, and XBB.1 variants.

Currently, SARS-CoV-2 variants of interest are XBB.1.5, XBB.1.16, BA.2.86, and some others (https://www.who.int/activities/tracking-SARS-CoV-2-variants/tracking-SARS-CoV-2-variants, 01.09.2024). A number of studies have shown a relatively close location of BA.2.86 and XBB.1.5 (distance of approximately 0.5-4 AU depending on the source of sera) [33-35]. Serum antibodies raised against XBB.1.5 cross-reacted with BA.2.86, supporting inclusion of XBB.1.5 in the updated vaccine.

COMPARISON OF "BASIC" ANTIGENIC MAPS WITH MAPS BUILT WITH SERA FROM VACCINED DONORS

By considering "basic" maps as a gold standard for determining virus antigenicity, we assume that the antibody response in humans and laboratory animals is generated in a similar way, although this is not entirely true. "Basic" antigenic maps can also be constructed using sera from donors who had been previously infected with a known SARS-CoV-2 variant. However, such sera will become increasingly difficult to obtain due to the increasing spread of hybrid immunity in the population. That is why it is important to build antigenic maps using the data from vaccinated donors and donors with the hybrid immunity and then to compare them with the "basic" maps.

In the study of the "pre-omicron" period [36], comparison of antigenic maps from the donors who had recovered from D614G or one of the SARS-CoV-2 variants, including the L452R variant, with the maps of those vaccinated with mRNA-1273 revealed the following differences. The distance between D614G and AY.1 (Delta family) on the map for the vaccinated individuals was greater than on the map for those who had recovered from the disease. D614G and Beta, on the contrary, were closer to each other. The Beta and AY.1 variants were located at a distance of about 1 AU on the map for the vaccinated individuals, while on the map of those who had recovered from the disease, they were more than 4 AU apart. The authors discovered a general trend that the studied variants D614G, Alpha, Beta, Kappa, Lambda, Delta, and others were located further from each other on the map for the recovered donors than on the map for vaccinated donors. The same observation was made in a more recent study that included donors who had recovered from COVID-19, including the Omicron BA.1 and BA.2 variants, as well as those who had received the mRNA-1273, BNT162b2, or AZD1222 vaccines [21]. On the map for the vaccinated individuals, D614G, Alpha, and Gamma were located almost in the same place and formed a cluster, while on the map of those who had recovered, the distance between these variants was about 1 AU. Another difference was location of sera on the maps. In the map of vaccinated individuals, the sera were located close to the D614G/Alpha/Gamma cluster only. On the map of those who had recovered from COVID-19, the sera were located closer to the variant that the donor had suffered from.

The study [21] also revealed differences in the positions of sera from the donors vaccinated with different vaccines. We noticed that the sera located near the D614G/Alpha/Gamma cluster, but closer to Omicron BA.1, were predominantly from the donors who received the mRNA-1273 vaccine. The sera from those vaccinated with BNT162b2 or AZD1222 were located near the D614G/Alpha/Gamma cluster and away from BA.1.

ANTIGENIC MAPS USED TO ASSESS THE DEVELOPMENT OF CROSS-REACTIVE ANTIBODIES AFTER BOOSTER VACCINATION

Comparison of antigenic maps before and after vaccination allows to monitor the formation of antibody

cross-reactivity. Booster vaccination leads to changes in the antigenic distances between the variants [20, 24, 37]. As an antigen used for serum testing remains constant, any variations in the antigenic distances between the variants are linked to changes in the composition of neutralizing antibodies in the sera. A decrease in the distance between two antigens may indicate that the serum contains more antibodies that bind to both antigens [38].

A number of studies have shown that the third booster vaccination with BNT162b2 leads to a decrease in the antigenic distance between D614G and BA.1, BA.2, BA2.12.1, and BA.4/5 [20, 24]. The same studies showed that after the third immunization with an mRNA vaccine, the antigenic distances between D614G and Delta, on the contrary, increased. We demonstrated that homologous booster vaccination with Sputnik-V leads to a decrease in the antigenic distance between WT and BA.1. We also found oppositely directed changes in the distances between WT and Delta after homo- and heterologous revaccination. Revaccination with Sputnik-V led to a decrease in the antigenic distance between WT and Delta, while vaccination with BNT162b2 increased this distance. These discrepancies may be due to the fact that Sputnik-V induces immune response to the full-length S protein, while BNT162b2 – to the pre-fusion stabilized conformation of the S protein [39-41].

Antigenic maps allow to quantify changes in the antigenic distances between the viral variants before and after vaccination. We proposed a convenient way to visualize these changes using the hat graphs [42]. The edge of the hat on such graph corresponds to the initial indicator value, i.e., to the antigenic distance between variants on the antigenic maps before the exposure. The height of the hat corresponds to the change in the antigenic distance, which can be either positive or negative (in the latter case the hat will be upside down). Using hat graphs, we visualized changes in the antigenic distances between WT and Alpha, Beta, Delta, Omicron BA.1, and BA.4/5 of the sera from volunteers revaccinated with Sputnik-V or BNT162b2 after primary vaccination with Sputnik-V [38]. The largest decrease in the antigenic distance occurred between WT and BA.1 for both types of booster vaccination.

ANTIBODY LANDSCAPES

The breadth of antibody response could be evaluated using an approach called antibody landscape modeling [43]. Antibody landscape represents a three-dimensional surface, where the *xy* plane is the “basic” antigenic map, and the height of the landscape (*z*-axis) is determined by the neutralization titer of sera of a studied group against a specific antigen. The smoothed surface is constructed using multiple linear regression. This creates an immunological profile of the sera with elevations corresponding to the areas on the antigenic map with higher levels of antibodies (Fig. 2).

Antibody landscapes constructed based on the data for cross-reactive sera are flatter, with less tilt

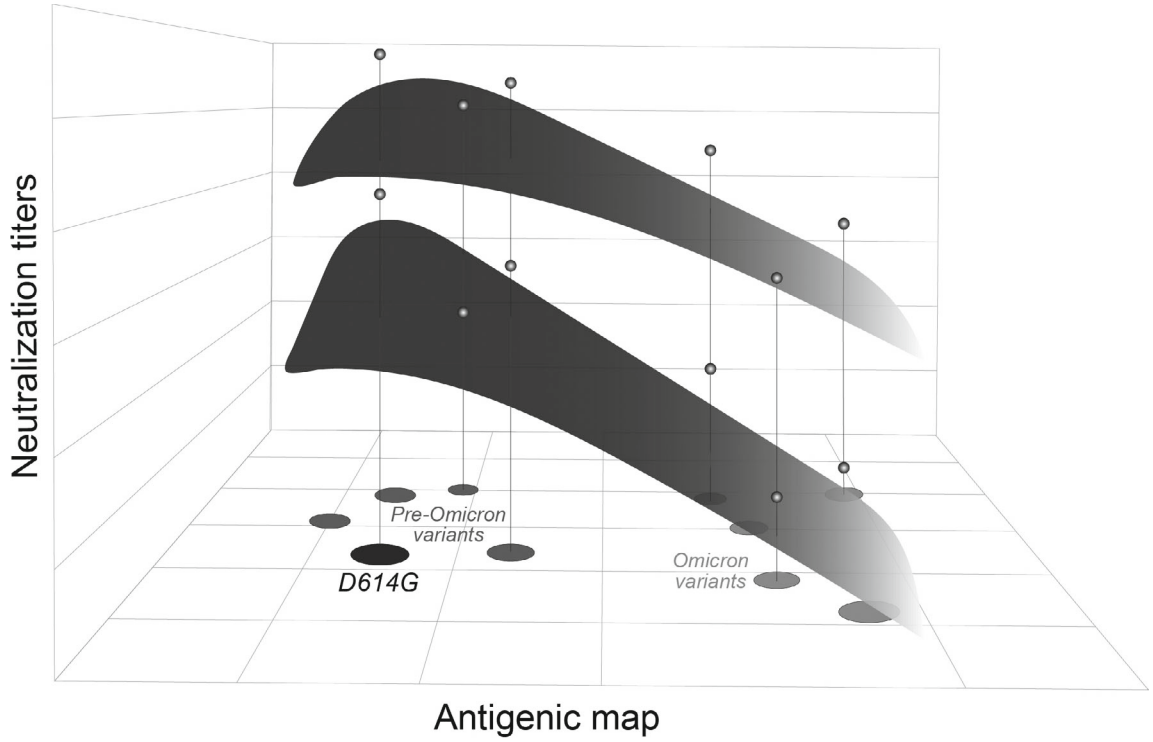

Fig. 2. Example of antibody landscapes (adapted from [32]).

towards one or another antigenic region (top landscape in Fig. 2). Antibody landscapes of individuals who had received two doses of mRNA-1273, BNT162b2, and AZD1222 vaccines, as well as of those who had been previously infected with the D614G, Alpha, and Beta variants, exhibit a distinct decline towards the Omicron cluster. This decline is attributed to the reduced neutralization titers of the Omicron variants compared to the pre-Omicron variants [19, 27]. Interestingly, the landscapes exhibited a flatter profile three months following double and triple booster with mRNA-1273, as compared to those obtained after one month [19], indicating that the decrease in the neutralization titer occurs at different rates – titers against pre-Omicron variants decreased faster, which may be due to rapid activation of memory B cells specific for pre-Omicron variants after booster immunization. The presence of specific antibodies produced by the plasma cells and activated memory B cells inhibits the development of naïve B cells with a similar specificity, on particular, through direct masking of dominant receptor-binding domain (RBD) epitopes [44]. However, naïve B cells do appear to be activated [45] and, during maturation in the germinal center, acquire a different specificity useful for neutralization of Omicron variants. By this moment, antibody secretion by memory B cells has already declined, so we see flatter antibody landscapes only 3 months after vaccination.

Flatter antibody landscapes were also observed in individuals with the hybrid immunity who have received bivalent (BA.1 or BA.4/5) vaccines, in contrast to the donors who had not been previously infected [32].

ASSESSING THE BREADTH OF NEUTRALIZATION USING ANTIGENIC CARTOGRAPHY

The concept of breadth of virus neutralization was introduced in the studies on the effectiveness of humoral immunity against several variants of SARS-CoV-2. This parameter shows how efficiently related and more distant variants of the virus are neutralized. As a rule, the breadth of virus neutralization is assessed qualitatively. However, we believe that antigenic cartography allows to quantify the breadth of virus neutralization.

Projecting 3D antibody landscapes on a plane produces a graph of the increase in the neutralization breadth [20]. The antigens are placed along the *x*-axis according to their antigenic distance (WT is typically taken as the reference point). The *y*-axis represents the neutralization titers of these antigens (Fig. 3). This type of graph allows to evaluate changes in the shape and area of the immune profile, which is especially useful when studying the dynamics of antibody response over a long period of time or after several vaccinations.

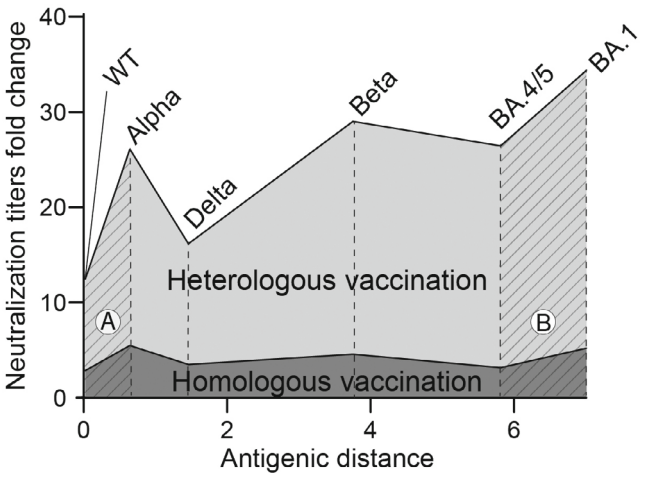

Fig. 3. Example of a graph of increasing neutralization breadth upon homo- and heterologous revaccination (adapted from [37]).

The changes in the shape of the immune profile on the breadth-gain plot can be assessed only qualitatively. It was shown that after triple vaccination with BNT162b2 or vaccination associated with BA.1 infection, there was a greater increase in the neutralization titers against variants antigenically distant from the vaccine strain [20].

Unlike shape, the area of the immune profile is a parameter that can be calculated quantitatively. However, a number of features should be taken into account. First, for the reasons described above, precise positioning of antigens on the *x*-axis is difficult. Second, the area will depend on the number of antigens against which the sera were tested. The two problems can be solved by standardization of methods used for the determination of the virus neutralization titers. Finally, it is important to consider that the greater the distance from the starting point along the *x*-axis, the more significant the contribution to the virus neutralization indicator. In this regard, to evaluate the area of each site, it is necessary to introduce a certain increasing factor, which, for example, for site B in Fig. 3 will be greater than for site A. As far as we know, a model for calculating the breadth of virus neutralization based on a graph of this type has not yet been developed.

CONCLUSION

Construction of antigenic maps has been traditionally used to choose a vaccine strain against the influenza virus [28] (https://www.who.int/publications/m/item/recommended-composition-of-influenza-virus-vaccines-

for-use-in-the-2023-2024-northern-hemisphere-influenza-season, 09.04.2023). Typically, antigenic maps confirm the findings of serological tests (e.g., virus neutralization) and are used to facilitate visualization of the obtained results. Thus, antigenic maps have clearly demonstrated that Omicron BA.1 and other variants of this family are antigenically distant from the ancestral variants of SARS-CoV-2 [19-25]. World Health Organization has incorporated these findings to support the necessity for the modification of coronavirus vaccine in order to accommodate new circulating strains (https://www.who.int/news/item/18-05-2023-statement-on-the-antigen-composition-of-covid-19-vaccines, 04.09.2023).

When choosing a new vaccine strain, it is crucial to select a strain whose antigenic characteristics would be significantly different from characteristics of the previous one. This helps reduce the impact of the "original sin," when previously generated memory B cells are preferentially activated in response to a new antigen instead of naïve B cells, which could produce more specific antibodies to the new antigen [45].

Using antigenic cartography, it was shown that variants of the Omicron family significantly differ in their antigenic characteristics not only from the ancestral forms of SARS-CoV-2, but also from each other. Analysis of antigenic maps revealed that infection with BA.5 produces an insufficient neutralizing response against BA.4.6, BA.5, XBB.1, and BQ.1.1 [25, 29]. Thus, bivalent BA.5-based vaccines were insufficiently effective against new variants [30-32]. The antigenic similarity of XBB.1.5 with the modern variant BA.2.86 that was shown using the antigenic maps, supports inclusion of XBB.1.5 in the updated vaccine [33-35]. Using antigenic characterization of the new variants, Food and Drug Administration (FDA) has recommended the development of a monovalent vaccine based on XBB.1.5 (https://www.fda.gov/vaccines-blood-biologics/updated-covid-19-vaccines-use-united-states-beginning-fall-2023, 01.09.2024).

Antigenic cartography and construction of antibody landscape allow to predict which viral variant can evade the formed immunity, i.e., to get ahead of the virus evolution and to prepare the vaccines in advance. Finally, antigen mapping provides an opportunity to quantitatively measure the breadth of virus neutralization by the sera.

Contributions. A.E.A. prepared the manuscript; A.A.M., Y.D.V., and A.V.F. edited the text.

Funding. This work was financially supported by the Russian Science Foundation (project no. 23-25-00472).

Ethics declarations. This work does not contain any studies involving human and animal subjects. The authors of this work declare that they have no conflicts of interest.

REFERENCES

1. Sun, C., Xie, C., Bu, G. L., Zhong, L. Y., and Zeng, M. S. (2022) Molecular characteristics, immune evasion, and impact of SARS-CoV-2 variants, *Signal Transduct. Target Ther.*, **7**, 202, doi: 10.1038/s41392-022-01039-2.
2. Tian, D., Sun, Y., Xu, H., and Ye, Q. (2022) The emergence and epidemic characteristics of the highly mutated SARS-CoV-2 Omicron variant, *J. Med. Virol.*, **94**, 2376-2383, doi: 10.1002/jmv.27643.
3. Guo, Y., Han, J., Zhang, Y., He, J., Yu, W., Zhang, X., Wu, J., Zhang, S., Kong, Y., Guo, Y., Lin, Y., and Zhang, J. (2022) SARS-CoV-2 Omicron variant: epidemiological features, biological characteristics, and clinical significance, *Front. Immunol.*, **13**, 877101, doi: 10.3389/fimmu.2022.877101.
4. Li, J., Lai, S., Gao, G. F., and Shi, W. (2021) The emergence, genomic diversity and global spread of SARS-CoV-2, *Nature*, **600**, 408-418, doi: 10.1038/s41586-021-04188-6.
5. Komissarov, A. B., Safina, K. R., Garushyants, S. K., Fadeev, A. V., Sergeeva, M. V., Ivanova, A. A., Danilenko, D. M., Lioznov, D., Shneider, O. V., Shvyrev, N., Spirin, V., Glyzin, D., Shchur, V., and Bazykin, G. A. (2021) Genomic epidemiology of the early stages of the SARS-CoV-2 outbreak in Russia, *Nat. Commun.*, **12**, 649, doi: 10.1038/s41467-020-20880-z.
6. Smith, D. J., Lapedes, A. S., De Jong, J. C., Bestebroer, T. M., Rimmelzwaan, G. F., Osterhaus, A. D. M. E., and Fouchier, R. A. M. (2004) Mapping the antigenic and genetic evolution of influenza virus, *Science*, **305**, 371-376, doi: 10.1126/science.1097211.
7. Tan, C. W., Chia, W. N., Qin, X., Liu, P., Chen, M. I.-C., Tiu, C., Hu, Z., Chen, V. C. W., Young, B. E., Sia, W. R., Tan, Y.-J., Foo, R., Yi, Y., Lye, D. C., Anderson, D. E., and Wang, L. F. (2020) A SARS-CoV-2 surrogate virus neutralization test based on antibody-mediated blockage of ACE2-spike protein-protein interaction, *Nat. Biotechnol.*, **38**, 1073-1078, doi: 10.1038/s41587-020-0631-z.
8. Astakhova, E. A., Byazrova, M. G., Yusubalieva, G. M., Larichev, V. F., Baklaushev, V. P., and Filatov, A. V. (2022) High heterogeneity of virus-neutralizing and RBD-binding activities of COVID-19 convalescent sera, *Mol. Biol.*, **56**, 1095-1103, doi: 10.1134/S002689332206005X.
9. Hyseni, I., Molesti, E., Benincasa, L., Piu, P., Casa, E., Temperton, N. J., Manenti, A., and Montomoli, E. (2020) Characterisation of SARS-CoV-2 lentiviral pseudotypes and correlation between pseudotype-based neutralisation assays and live virus-based micro neutralisation assays, *Viruses*, **12**, 1011, doi: 10.3390/v12091011.
10. Schmidt, F., Weisblum, Y., Muecksch, F., Hoffmann, H. H., Michailidis, E., Lorenzi, J. C. C., Mendoza, P., Rutkowska, M., Bednarski, E., Gaebler, C., Agudelo, M., Cho, A., Wang, Z., Gazumyan, A., Cipolla, M., Caskey, M., Robbiani, D. F., Nussenzweig, M. C., Rice, C. M.,

Hatziioannou, T., and Bieniasz, P. D. (2020) Measuring SARS-CoV-2 neutralizing antibody activity using pseudotyped and chimeric viruses, *J. Exp. Med.*, **217**, e20201181, doi: 10.1084/jem.20201181.

11. Saeys, Y., Van Gassen, S., and Lambrecht, B. N. (2016) Computational flow cytometry: Helping to make sense of high-dimensional immunology data, *Nat. Rev. Immunol.*, **16**, 449-462, doi: 10.1038/nri.2016.56.
12. Dorrity, M. W., Saunders, L. M., Queitsch, C., Fields, S., and Trapnell, C. (2020) Dimensionality reduction by UMAP to visualize physical and genetic interactions, *Nat. Commun.*, **11**, 1537, doi: 10.1038/s41467-020-15351-4.
13. Becht, E., McInnes, L., Healy, J., Dutertre, C. A., Kwok, I. W. H., Ng, L. G., Ginhoux, F., and Newell, E. W. (2019) Dimensionality reduction for visualizing single-cell data using UMAP, *Nat. Biotechnol.*, **37**, 38-47, doi: 10.1038/nbt.4314.
14. Van der Maaten, L., and Hinton, G. (2008) Visualizing data using t-SNE, *J. Mach. Learn. Res.*, **9**, 2579-2605.
15. Mcinnes, L., Healy, J., and Melville, J. (2021) UMAP: Uniform Manifold Approximation and Projection for dimension reduction, *arXiv*, doi: 10.48550/arXiv.1802.03426.
16. Cai, Z., Zhang, T., and Wan, X. (2012) Antigenic distance measurements for seasonal influenza vaccine selection, *Vaccine*, **30**, 448-453, doi: 10.1016/j.vaccine.2011.10.051.
17. Amanat, F., Strohmeier, S., Meade, P., Dambrauskas, N., Mühlemann, B., Smith, D. J., Vigdorovich, V., Noah Sather, D., Coughlan, L., and Krammer, F. (2021) Vaccination with SARS-CoV-2 variants of concern protects mice from challenge with wild-type virus, *PLoS Biol.*, **19**, e3001384, doi: 10.1371/journal.pbio.3001384.
18. Mykytyn, A. Z., Rissmann, M., Kok, A., Rosu, M. E., Schipper, D., Breugem, T. I., van den Doel, P. B., Chandler, F., Bestebroer, T., de Wit, M., van Royen, M. E., Molenkamp, R., Oude Munnink, B. B., de Vries, R. D., GeurtsvanKessel, C., Smith, D. J., Koopmans, M. P. G., Rockx, B., Lamers, M. M., Fouchier, R. A. M., and Haagmans, B. L. (2022) Antigenic cartography of SARS-CoV-2 reveals that Omicron BA.1 and BA.2 are antigenically distinct, *Sci. Immunol.*, **7**, eabq4450, doi: 10.1126/sciimmunol.abq4450.
19. Wilks, S. H., Mühlemann, B., Shen, X., Türeli, S., LeGresley, E. B., Netzl, A., Caniza, M. A., Chacaltana-Huarcaya, J. N., Corman, V. M., Daniell, X., Datto, M. B., Dawood, F. S., Denny, T. N., Drosten, C., Fouchier, R. A. M., Garcia, P. J., Halfmann, P. J., Jassem, A., Jeworowski, L. M., Jones, T. C., Kawaoka, Y., Krammer, F., McDanal, C., Pajon, R., Simon, V., Stockwell, M. S., Tang, H., van Bakel, H., Veguilla, V., Webby, R., Montefiori, D. C., and Smith, D. J. (2023) Mapping SARS-CoV-2 antigenic relationships and serological responses, *Science*, **382**, eadj0070, doi: 10.1126/science.adj0070.
20. Wang, W., Lusvarghi, S., Subramanian, R., Epsi, N. J., Wang, R., Goguet, E., Fries, A. C., Echegaray, F., Vassell, R., Coggins, S. A., Richard, S. A., Lindholm, D. A., Mende, K., Ewers, E. C., Larson, D. T., Colombo, R. E., Colombo, C. J., Joseph, J. O., Rozman, J. S., Smith, A., Lalani, T., Berjohn, C. M., Maves, R. C., Jones, M. U., Mody, R., Huprikar, N., Livezey, J., Saunders, D., Hollis-Perry, M., Wang, G., Ganesan, A., Simons, M. P., Broder, C. C., Tribble, D. R., Laing, E. D., Agan, B. K., Burgess, T. H., Mitre, E., Pollett, S. D., Katzelnick, L. C., and Weiss, C. D. (2022) Antigenic cartography of well-characterized human sera shows SARS-CoV-2 neutralization differences based on infection and vaccination history, *Cell Host Microbe*, **30**, 1745-1758.e7, doi: 10.1016/j.chom.2022.10.012.
21. Van der Straten, K., Guerra, D., van Gils, M. J., Bontjer, I., Caniels, T. G., van Willigen, H. D. G., Wynberg, E., Poniman, M., Burger, J. A., Bouhuijs, J. H., van Rijswijk, J., Olijhoek, W., Liesdek, M. H., Lavell, A. H. A., Appelman, B., Sikkens, J. J., Bomers, M. K., Han, A. X., Nichols, B. E., Prins, M., Vennema, H., Reusken, C., de Jong, M. D., de Bree, G. J., Russell, C. A., Eggink, D., and Sanders, R. W. (2022) Antigenic cartography using sera from sequence-confirmed SARS-CoV-2 variants of concern infections reveals antigenic divergence of Omicron, *Immunity*, **55**, 1725-1731.e4, doi: 10.1016/j.immuni.2022.07.018.
22. Mühlemann, B., Trimpert, J., Walper, F., and Schmidt, M. L. (2023) Antigenic cartography using variant-specific hamster sera reveals substantial antigenicv among Omicron subvariants, *bioRxiv*, doi: 10.1101/2023.07.02.547076.
23. Bekliz, M., Adea, K., Vetter, P., Eberhardt, C. S., Hosszu-Fellous, K., Vu, D. L., Puhach, O., Essaidi-Laziosi, M., Waldvogel-Abramowski, S., Stephan, C., L'Huillier, A. G., Siegrist, C. A., Didierlaurent, A. M., Kaiser, L., Meyer, B., and Eckerle, I. (2022) Neutralization capacity of antibodies elicited through homologous or heterologous infection or vaccination against SARS-CoV-2 VOCs, *Nat. Commun.*, **13**, 3840, doi: 10.1038/s41467-022-31556-1.
24. Lusvarghi, S., Pollett, S. D., Neerukonda, S. N., Wang, W., Wang, R., Vassell, R., Epsi, N. J., Fries, A. C., Agan, B. K., Lindholm, D. A., Colombo, C. J., Mody, R., Ewers, E. C., Lalani, T., Ganesan, A., Goguet, E., Hollis-Perry, M., Coggins, S. A., Simons, M. P., Katzelnick, L. C., Wang, G., Tribble, D. R., Bentley, L., Eakin, A. E., Broder, C. C., Erlandson, K. J., Laing, E. D., Burgess, T. H., Mitre, E., and Weiss, C. D. (2022) SARS-CoV-2 BA.1 variant is neutralized by vaccine booster-elicited serum but evades most convalescent serum and therapeutic antibodies, *Sci. Transl. Med.*, **14**, 8543, doi: 10.1126/scitranslmed.abn8543.
25. Mykytyn, A. Z., Rosu, M. E., Kok, A., Rissmann, M., van Amerongen, G., Geurtsvankessel, C., de Vries, R. D., Munnink, B. B. O., Smith, D. J., Koopmans, M. P. G.,

Lamers, M. M., Fouchier, R. A. M., and Haagmans, B. L. (2023) Antigenic mapping of emerging SARS-CoV-2 omicron variants BM.1.1.1, BQ.1.1, and XBB.1, *Lancet Microbe*, **4**, e294-e295, doi: 10.1016/S2666-5247(22)00384-6.

26. Wang, X., Jiang, S., Jiang, S., Li, X., Ai, J., Lin, K., Lv, S., Zhang, S., Li, M., Li, J., Dai, L., Hu, Z., Zhang, W., Zhang, Y., and Wang, P. (2023) Neutralization of SARS-CoV-2 BQ.1.1, CH.1.1, and XBB.1.5 by breakthrough infection sera from previous and recent waves in China, *Cell Discov.*, **9**, 5-8, doi: 10.1038/s41421-023-00569-5.
27. Rössler, A., Netzl, A., Knabl, L., Schäfer, H., Wilks, S. H., Bante, D., Falkensammer, B., Borena, W., von Laer, D., Smith, D. J., and Kimpel, J. (2022) BA.2 and BA.5 omicron differ immunologically from both BA.1 omicron and pre-omicron variants, *Nat. Commun.*, **13**, 7701, doi: 10.1038/s41467-022-35312-3.
28. Fouchier, R. A. M., and Smith, D. J. (2010) Use of antigenic cartography in vaccine seed strain selection, *Avian Dis.*, **54**, 220-223, doi: 10.1637/8740-032509-ResNote.1.
29. Xia, H., Yeung, J., Kalveram, B., Bills, C. J., Chen, J. Y. C., Kurhade, C., Zou, J., Widen, S. G., Mann, B. R., and Kondor, R. (2023) Cross-neutralization and viral fitness of SARS-CoV-2 Omicron sublineages, *Emerg. Microbes Infect.*, **12**, e2161422, doi: 10.1080/22221751.2022.2161422.
30. Kurhade, C., Zou, J., Xia, H., Liu, M., Chang, H. C., Ren, P., Xie, X., and Shi, P. Y. (2023) Low neutralization of SARS-CoV-2 Omicron BA.2.75.2, BQ.1.1 and XBB.1 by parental mRNA vaccine or a BA.5 bivalent booster, *Nat. Med.*, **29**, 344-347, doi: 10.1038/s41591-022-02162-x.
31. Hoffmann, M., Behrens, G. M. N., Arora, P., Kempf, A., Nehlmeier, I., Cossmann, A., Manthey, L., Dopfer-Jablonka, A., and Pöhlmann, S. (2022) Effect of hybrid immunity and bivalent booster vaccination on Omicron sublineage neutralization, *Lancet*, **23**, 25-28, doi: 10.1016/S1473-3099(22)00792-7.
32. Roessler, A., Netzl, A., Knabl, L., Bante, D., Wilks, S. H., Borena, W., Laer, D. vo., Smith, D. J., and Kimpel, J. (2023) Characterizing SARS-CoV-2 neutralization profiles after bivalent boosting using antigenic cartography, *Nat. Commun.*, **14**, 5224, doi: 10.1038/s41467-023-41049-4.
33. Coombes, N., Bewley, K. R., Duff, Y. L., Alami-Rahmouni, N., Ryan, K. A., Kempster, S., Ferguson, D., Davies, E. R., Weldon, T. M., and Cross Eleanor, S. (2023) Evaluation of the neutralising antibody response in human and hamster sera against SARS-CoV-2 variants up to and including BA.2.86 using an authentic virus neutralisation assay, *bioRxiv*, doi: 10.1101/2023.10.21.563398.
34. Qu, P., Xu, K., Faraone, J. N., Goodarzi, N., Zheng, Y.-M., Carlin, C., Bednash, J. S., Horowitz, J. C., Mallampall, R. K., and Saif, L. J. (2023) Immune evasion, infectivity, and fusogenicity of SARS-CoV-2 Omicron BA.2.86 and flip variants, *bioRxiv*, doi: 10.1101/2023.09.11.557206.
35. Ba, S., Ho, J., Zhang, R. M., Iketani, S., Yu, J., Huang, Y., and Qu, Y. (2023) Antigenicity and receptor affinity of SARS-CoV-2 BA.2.86 spike, *Nature*, **624**, 639-644, doi: 10.1038/s41586-023-06750-w.
36. Neerukonda, S. N., Vassell, R., Lusvarghi, S., Wang, R., Echegaray, F., Bentley, L., Eakin, A. E., Erlandson, K. J., Katzelnick, L. C., Weiss, C. D., and Wang, W. (2021) SARS-CoV-2 Delta variant displays moderate resistance to neutralizing antibodies and Spike protein properties of higher soluble ACE2 sensitivity, enhanced cleavage and fusogenic activity, *Viruses*, **13**, 2485, doi: 10.3390/v13122485.
37. Astakhova, E. A., Morozov, A. A., Byazrova, M. G., Sukhova, M. M., Mikhailov, A. A., Minnegalieva, A. R., Gorchakov, A. A., and Filatov, A. V. (2023) Antigenic cartography indicates that the Omicron BA.1 and BA.4/BA.5 variants remain antigenically distant to ancestral SARS-CoV-2 after Sputnik V vaccination followed by homologous (Sputnik V) or heterologous (Comirnaty) revaccination, *Int. J. Mol. Sci.*, **24**, 10493, doi: 10.3390/ijms241310493.
38. Anderson, C. S., Sangster, M. Y., Yang, H., Mariani, T. J., Chaudhury, S., and Topham, D. J. (2020) Implementing sequence-based antigenic distance calculation into immunological shape space model, *BMC Bioinformatics*, **21**, 256, doi: 10.1186/s12859-020-03594-3.
39. Anderson, E. J., Rouphael, N. G., Widge, A. T., Jackson, L. A., Roberts, P. C., Makhene, M., Chappell, J. D., Denison, M. R., Stevens, L. J., Pruijssers, A. J., McDermott, A. B., Flach, B., Lin, B. C., Doria-Rose, N. A., O'Dell, S., Schmidt, S. D., Corbett, K. S., Swanson, P. A., Padilla, M., Neuzil, K. M., Bennett, H., Leav, B., Makowski, M., Albert, J., Cross, K., Edara, V. V., Floyd, K., Suthar, M. S., Martinez, D. R., Baric, R., Buchanan, W., Luke, C. J., Phadke, V. K., Rostad, C. A., Ledgerwood, J. E., Graham, B. S., and Beigel, J. H. (2020) Safety and immunogenicity of SARS-CoV-2 mRNA-1273 vaccine in older adults, *N. Engl. J. Med.*, **383**, 2427-2438, doi: 10.1056/NEJMoa2028436.
40. Walsh, E. E., Frenck, R. W., Falsey, A. R., Kitchin, N., Absalon, J., Gurtman, A., Lockhart, S., Neuzil, K., Mulligan, M. J., Bailey, R., Swanson, K. A., Li, P., Koury, K., Kalina, W., Cooper, D., Fontes-Garfias, C., Shi, P.-Y., Türeci, Ö., Tompkins, K. R., Lyke, K. E., Raabe, V., Dormitzer, P. R., Jansen, K. U., Şahin, U., and Gruber, W. C. (2020) Safety and immunogenicity of two RNA-based COVID-19 vaccine candidates, *N. Engl. J. Med.*, **383**, 2439-2450, doi: 10.1056/NEJMoa2027906.
41. Logunov, D. Y., Dolzhikova, I. V., Zubkova, O. V., Tukhvatullin, A. I., Shcheblyakov, D. V., Dzharullaeva, A. S., Grousova, D. M., Erokhova, A. S., Kovyrshina, A. V., Botikov, A. G., Izhaeva, F. M., Popova, O., Ozharovskaya, T. A., Esmagambetov, I. B., Favorskaya, I. A., Zrelkin, D. I., Voronina, D. V., Shcherbinin, D. N., Semikhin, A. S.,

Simakova, Y. V., Tokarskaya, E. A., Lubenets, N. L., Egorova, D. A., Shmarov, M. M., Nikitenko, N. A., Morozova, L. F., Smolyarchuk, E. A., Kryukov, E. V., Babira, V. F., Borisevich, S. V., Naroditsky, B. S., and Gintsburg, A. L. (2020) Safety and immunogenicity of an rAd26 and rAd5 vector-based heterologous prime-boost COVID-19 vaccine in two formulations: two open, non-randomised phase 1/2 studies from Russia, *Lancet*, **396**, 887-897, doi: 10.1016/S0140-6736(20)31866-3.

42. Witt, J. K. (2019) Introducing hat graphs, *Cogn. Res. Princ. Implic.*, **4**, 31, doi: 10.1186/s41235-019-0182-3.
43. Fonville, J. M., Wilks, S. H., James, S. L., Fox, A., Ventresca, M., Aban, M., Xue, L., Jones, T. C., Le, N. M. H., Pham, Q. T., Tran, N. D., Wong, Y., Mosterin, A., Katzelnick, L. C., Labonte, D., Le, T. T., Van Der Net, G., Skepner, E., Russell, C. A., Kaplan, T. D., Rimmelzwaan, G. F., Masurel, N., De Jong, J. C., Palache, A., Beyer, W. E. P., Le, Q. M., Nguyen, T. H., Wertheim, H. F. L., Hurt, A. C., Osterhaus, A. D. M. E., Barr, I. G., Fouchier, R. A. M., Horby, P. W., and Smith, D. J. (2014) Antibody landscapes after influenza virus infection or vaccination, *Science*, **346**, 996-1000, doi: 10.1126/science.1256427.
44. Schaefer-Babajew, D., Wang, Z., Muecksch, F., Cho, A., Loewe, M., Cipolla, M., Raspe, R., Johnson, B., Canis, M., DaSilva, J., Ramos, V., Turroja, M., Millard, K. G., Schmidt, F., Witte, L., Dizon, J., Shimeliovich, I., Yao, K. H., Oliveira, T. Y., Gazumyan, A., Gaebler, C., Bieniasz, P. D., Hatziioannou, T., Caskey, M., and Nussenzweig, M. C. (2023) Antibody feedback regulates immune memory after SARS-CoV-2 mRNA vaccination, *Nature*, **613**, 735-742, doi: 10.1038/s41586-022-05609-w.
45. Schiepers, A., van 't Wout, M. F. L., Greaney, A. J., Zang, T., Muramatsu, H., Lin, P. J. C., Tam, Y. K., Mesin, L., Starr, T. N., Bieniasz, P. D., Pardi, N., Bloom, J. D., and Victora, G. D. (2023) Molecular fate-mapping of serum antibody responses to repeat immunization, *Nature*, **615**, 482-489, doi: 10.1038/s41586-023-05715-3.